Computers Math. Applic. Vol. 22, No. 6, pp. 29–45, 1991
Printed in Great Britain.

0097-4943/91 $3.00 + 0.00

ASYMPTOTIC STABILITY AND QUASI-PERIODICITY IN FORM AND EVOLUTION OF MODEL SOCIO-SPATIAL STRUCTURES

DIMITRIOS S. DENDRINOS[1,2]
Urban and Transportation Dynamics Laboratory, Transportation Center
The University of Kansas, Lawrence, Kansas 66045, USA

(Received April 1990)

Abstract—This paper explores three particular cases of attractors in the three-location one-stock version of a universal map of discrete relative socio-spatial model dynamics. These specific cases are studied because they belong to certain basic families of dynamical motion. They are found in a small neighborhood of the map's parameter space, each resulting from the other by changing a single parameter.

Of the three attractors, two belong to the quasi-periodic species, whereas the third identifies a complex point attractor with fractal properties. The cases document the universality of the deterministic map. For example, the Curry-Yorke toroidal flow of a quasi-periodic attractor in absolute dynamics is shown to be present here. Cyclical asymptotic stability, toroidal flow and their transition to chaos are only some of the many events contained in the universal map.

1. INTRODUCTION: CHAOS IN SOCIO-SPATIAL DYNAMICS

It is now accepted that turbulence in model dynamics is quite common. When the full range of the parameter space is explored in a broad range of discrete or continuous kinetic equations, some form of chaos or quasi-periodicity is likely to occur. Interesting, novel and unexpected events may hide in these dynamics, and new insights into the nature of evolution may lurk in them. The advent of bifurcation theory and the study of model chaos has triggered new developments in this field of mathematics and in a number of areas in the natural and biological sciences. The advances have now made inroads into the social sciences, as well.

Human population and other social stocks, it has been argued in the past, do not behave like fluids or air masses, substances commonly associated with turbulence. It was assumed that high transaction and transportation costs in spatio-temporal movements of social stocks prevent chaotic motions. Skeptics question whether chaos theory is relevant to model socio-spatial dynamics, considering the possibility that chaotic movements may simply be mathematical oddities. Social systems were perceived as dynamically stable. There must have been at least some stability in order for the systems to function, to be observed, and for learning about them to take place.

The strength of these arguments is now widely presumed to have diminished considerably. First, spatial barriers including political jurisdictions and the variety of topographical features encountered in space, as well as climatic conditions and other factors, do not inhibit turbulence. These are elements largely impeding the smooth, continuous and periodic spatial movement of human populations and other social stocks like capital, output, information, etc. They enhance the potential for chaotic motion. Dynamic models of spatial interaction involving congestion now demonstrate that, when transaction costs are included turbulence may occur, [1–3].

[1]The author wishes to acknowledge the contribution of his Research Assistants Jian Zhang and Bo Guo for help in carrying out the computer analysis.
[2]A version of this paper was presented at the November, 1989 Meeting of the Italian Regional Science Association in Rome.

Second, chaotic and quasi-periodic dynamics are not mathematical oddities. They are found in many dynamic specifications of socio-spatial systems, see for example [1, 4–8]. Even in long standing economic models chaotic events have been shown to be present under specific conditions [9,10]. A casual look at the stock market must convince these skeptics. Real, as opposed to simply model chaos, characterizes stock prices.

Third, and most serious, is the criticism of turbulence models in social sciences based on the contention that only stable events can be observed, having survived a process of selection which has eliminated unstable or chaotic patterns; and that only in stable and periodic systems learning or speculation can occur. To this argument one can counter with the following arguments at least. First, what is dynamically stable or periodic within a time frame may not be stable in a longer time period. Second, what is seemingly unstable in a short time period may be stable in a longer time frame. Third, unstable, quasi-periodic or chaotic behavior can be informative in some statistical sense. Fourth, socio-spatial systems perceived as stable may only be so in a very aggregate (or average) sense, whereas at a more disaggregated level, stability may be elusive or break down. Fifth, the definition of "stable" and "unstable" dynamics needs refinement, particularly so when quasi-periodicity is involved. Sixth, the socio-spatial selection principle may often favor unstable rather than stable patterns, or at least a combination of both, judging from a variety of unstable socio-spatial events observed over centuries of human history.

Most of the exposition here addresses issues of analytical rather than substantive interest. Nonetheless, the implications these findings hold for socio-spatial analysis are significant. As all three cases presented here identify some sort of dynamically stable behavior, the point is made that the road to such stability may hide, in some instances, seemingly unstable (among them, quasi-periodic) paths.

In most cases one can associate, in a one-to-one manner, the end-states with the parameter values set responsible for them. In most, but not all, instances starting values do not matter. In a few instances, starting position plays a significant role in the dynamic path, as it may belong to different basins of attraction in the phase portrait. So far, in the universal map of socio-spatial dynamics presented here, at most two different basins of attraction have been detected in the phase portrait. Evidence seems to indicate that their boundary is not fractal.

An exhaustive numerical search into the universe of the map's parameters and initial values space will reveal the whole extent of families, species, and their sub-species of dynamics hidden in the map. Once this catalogue has been derived, one may be more confident in deriving conclusions about the local or global occurrence of specific socio-spatial dynamics, and their statistical frequency.

Finally, in what follows, the preoccupation is not with formal mathematical proof, left to the interested mathematician. Instead, the emphasis is on the recording of the phenomena encountered of potential interest to social scientists.

2. FORM, STRUCTURE AND QUASI-CHAOS

A variety of quasi-periodic motion is produced by the universal map. Deterministic transition from periodicity to quasi-periodicity, or from quasi-periodic movement to chaos, provides clues as to their inner structure. Beyond the novelty of the menu of chae and toroidal flows uncovered, core properties found in the time-one maps, their Poincaré sections and corresponding circle maps are revealed.

The evolution of geometry-geography in socio-spatial dynamics replicates certain patterns found in nature and their changing structure. Often creating new forms, this geometry-geography contains morphogenetic principles. These principles are based on the strong feedback iterative dynamics of the maps, which reveal stunning forms of order in asymptotically stable, quasi-periodic and chaotic motions.

Dynamics of human, animal and plant species populations trace abstract forms in a phase portrait. As recorded at various locations of the heterogeneous and non isotropic space that these stocks have occupied in time, their interactive dynamics generate patterns observed in other contexts. A general process has been suggested to approximate (model) them: a universal discrete map of socio-spatial relative dynamics. Consequently, reading of this paper requires prior exposure to this map, as well as to the theory of chaos.

This paper is not so much on the arguments for the applicability of the universal map. To the arguments already supplied in previous papers by this author and others, this paper adds nothing new. Instead, this paper focuses on the novel, and at times striking, geometry this map creates. It is, to an extent, an exploration in the pure aesthetics of form in socio-spatial model dynamics.

The universal map produces certain non-random, often robust and frequently repeated, elementary forms of quasi-periodicity and chaos. A number of these elementary forms, when projected onto a three-dimensional space, share common and strong phenomenological similarities to certain three-dimensional structures widely observed in nature. Three specific structures are analyzed in this paper, one in cyclical asymptotic stability, and two in quasi-periodicity, none in chaos however. The latter is left to forthcoming publications.

It is uncovered that giving rise to these asymptotically stable and quasi-periodic forms is a non-regular but periodic oscillation associated with a rotating periodicity. The arithmetic diffeomorphisms found in this irregular cyclical movement supply a morphogenetic principle. This form-generating principle has a variety of manifestations at different parts of the model's parameter space. A unifying developmental and evolutionary mechanism of morphogenesis is potentially derived. It is partly based on the inter-locking principle of quasi-periodicity, one of the core evolutionary principles involving elementary forms and fundamental bifurcations in iterative (discrete) maps.

Succession of iterates, for a particular starting state and a parameter set, produces the development of an elementary form. Sequences of trajectories, in a series of phase portraits (forms) corresponding to a travel in parameter space and starting values, supply snapshots of a deterministic sequence among stable, quasi-periodic and chaotic dynamics. This sequence records a deterministic path in the evolution of form. A menu of conditions may be studied corresponding to different time lags and periodic forcing. Systematic variation in such conditions reveals systematic transformations in the map's multifaceted dynamics. Succession of time lags and periods reveal an underlying mechanism in the map's inherent multiplicity of forms, some of them resembling observed structures in nature. The so called "rotation number" of circle maps (see Appendix) is one index to describe such forms. In all, new views of the socio-spatial world emerge, bearing similarities to those of the natural world.

Successive time lags and/or periodic forcing unravel and break down into its constituent parts the order found in these quasi-periodic movements. Thus, they reveal the inner and multifaceted structure of quasi-periodicity and its transformation from a starting, potentially stable, state to an, eventually, chaotic end-state. One might hint that natural form may be the product of quasi-periodicity.

3. THE UNIVERSAL MAP OF SOCIO-SPATIAL DYNAMICS

A universal mechanism of choice among mutually exclusive and competing alternatives involving a one-time-period-delay effect is the Dendrinos-Sonis map of socio-spatial relative dynamics. The statement of the I-alternatives (in this case, I different locations) and one-stock (a homogenous population) version of the map is:

$$x_i(t+1) = \frac{F_i(t)}{\sum_{j=1}^{I} F_j(t)}, \qquad i = 1, 2, \ldots, I, \tag{1}$$

$$F_i(t) = F_i\,[x_i(t);\ i = 1, 2, \ldots, I] > 0, \tag{2}$$

$$0 < x_i(0) < 1, \tag{3}$$

$$\sum_{i=1}^{I} x_i(0) = 1, \tag{4}$$

so that:

$$0 < [x_i(t), x_i(t+1)] < 1, \tag{5}$$

$$\sum_{i=1}^{I} x_i(t+1) = 1. \tag{6}$$

The specific version which is to be discussed in this paper is the three-location (heterogenous space), one-stock problem, where:

$$F_i(t) = A \prod_{k=1}^{3} x_k{}^{a_{ik}}, \qquad i = 1,2,3, \tag{7}$$

$$-\infty \leq a_{ik} \leq +\infty, \qquad i,k = 1,2,3, \tag{8}$$

$$A_i > 0, \qquad i = 1,2,3. \tag{9}$$

Functions F_i depict the current (at t) advantages of alternative location i, deterministically forcing a corresponding proportional choice (response) at the next time period (iteration) $t+1$, assuming one period response lag in real time.

Parameter set A' depicts the effects of the environment upon any of these locations. They are "scale," and slow moving, bifurcation parameters in the model. The exponents set $[a]$ pick up the comparative locational advantages elasticities with respect to the current population sizes, involving transaction (transportation among other) costs. They are given by:

$$\frac{\partial F_i(t)}{\partial x_k(t)} \Big/ \frac{F_i(t)}{x_k(t)} = a_{ik}, \tag{10}$$

and they identify very slow moving bifurcation parameters.

The behavior of the map has been extensively analyzed in past publications. For a complete set of references, the reader is directed to the corresponding citations found in [11]. Three specific points in the parameter space of the above specifications are the focus of the analysis to follow. These specifications are supplied in the Appendix, together with a documentation of how the computer generated graphs were obtained.

Three cases of dynamic motion are presented next. Time-one maps of the three-location one-stock problem have, at any point in the $[(t+1)$ vs. $t]$ space, slopes given by the Jacobian matrix:

$$s_{ij}(t+1,t) = \frac{x_i(t+1)}{x_j(t)} \left[a_{ij} - x_j(t) \sum_{h=1}^{3} a_{hi} \frac{A_h}{A_i} \prod_{m} x_m(t)^{(a_{hm} - a_{im})} \right], \tag{11}$$

for $i,j = 1,2,3$. These nine entries, which drive the time-one dynamics of the iterative process, are computed under the parameter specifications supplied in the Appendix, for each of the three cases. Beyond the parameters involved in the model specifications, the initial conditions $[x_i(0); i = 1,2,3]$ have, at times, a significant effect upon the map's dynamics in the phase portrait. This effect is documented in each of the three cases examined.

It becomes apparent, from the analysis which follows, that these cases are examples of a broad class of forms associated with fundamental three-dimensional dynamics. Further, these elementary dynamical forms seem to be the result of fundamental bifurcations occurring in the discrete three-dimensional relative dynamics. These fundamental bifurcations are qualitatively equivalent to the Hopf bifurcation in continuous, two dimensional, absolute dynamics and to the "flip" bifurcation, see [12]. This particular bifurcation has been analyzed in detail by Dendrinos and Sonis [11], in reference to the discrete two-dimensional relative dynamics bifurcations.

Although two of the three types of dynamics presented here are labeled as quasi-periodic, they, in part, result in stable non-random spatio-temporal structures. How they get to generate these structures, given some arbitrary initial perturbation, and the choreography of their iterative process (i.e., their full histories) is of great interest. By looking at how these structures are

formed, one obtains clues on core elementary processes at work in evolution. Thus, part of the vail from model chaos is shed and one can look directly into it.

In [11], the emphasis was on the bifurcations found by examining changes in the environmental (slowly changing) parameters [A]. Here, the focus is on bifurcations resulting from changes in the initial conditions and in the, relatively, very slowly altered exponents [a] of the universal map. It is underlined that all cases discussed next present one starting value and one path motions on the phase portrait (the Möbius triangle).

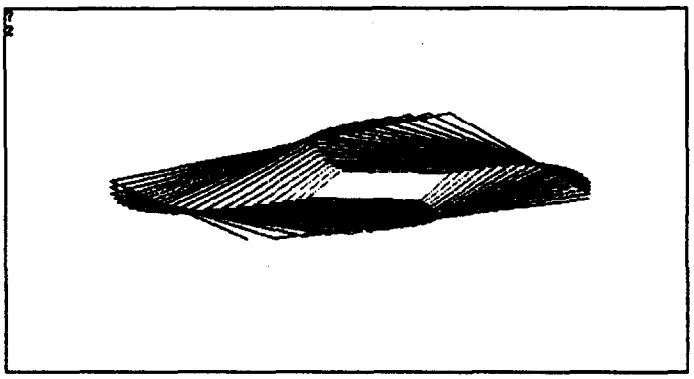

Figure 1. The formation of an attractor-ring with quasi-periodic motion: starting values inside the ring.

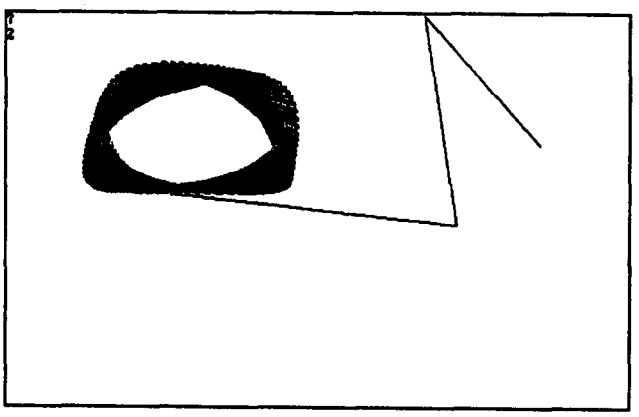

Figure 2. A ring-attractor when starting values are outside the ring.

4. RECTANGULAR RING

In Figure 1 the form of a ring type, quasi-periodic attractor is shown, when lines are plotted and the initial values are inside the ring. In Figure 2 the attractor is shown when the starting state is outside the ring. The precise kinetic equations of the discrete movement are supplied in the Appendix and the initial perturbation is $[x_1(0) = 0.2, \quad x_2(0) = 0.5, \quad x_3(0) = 0.3]$. A well defined ring structure takes shape without any fractal dimension on it. Location, shape and size of the ring do not vary as the starting point moves in the phase portrait, which is defined by the Möbius triangle in the three-location case. Symmetrically placed bands of motion characterize the ring-attractor.

Next time period responses of this version of the map are given by:

$$s_{ij}(t+1,t) = \frac{\partial x_i(t+1)}{\partial x_j(t)}; \qquad i,j = 1,2,3. \tag{13}$$

These slope-responses, evaluated at equilibrium, are the entries of the Jacobian matrix $J^* = [s^*_{ij}]$.

Specifically, the s_{ij} and s^*_{ij} entries are:

$$s_{11}(t+1,t) = x_1(t+1)^2\,[-1.5\,x_1(t)^{0.5}\,x_2(t)^{1.5}\,x_3(t)^{-1.5} + 0.015\,x_1(t)^{-2.5}\,x_3(t)^{-1.5}], \tag{14.1}$$

$$s_{12}(t+1,t) = -x_1(t+1)^2\,[1.5\,x_1(t)^{1.5}\,x_2(t)^{0.5}\,x_3(t)^{-1.5}], \tag{14.2}$$

$$s_{13}(t+1,t) = x_1(t+1)^2\,[1.5\,x_1(t)^{1.5}\,x_2(t)^{1.5}\,x_3(t)^{-2.5} + 0.015\,x_1(t)^{-1.5}x_3(t)^{-2.5}], \tag{14.3}$$

$$s_{21}(t+1,t) = \frac{x_2(t+1)}{x_1(t)}\,[1.5 - x_2(t+1)\,\{1.5 - 0.015\,x_1(t)^{-3}\,x_2(t)^{-1.5}\}], \tag{14.4}$$

$$s_{22}(t+1,t) = 1.5\,\frac{x_2(t+1)}{x_2(t)}, \tag{14.5}$$

$$s_{23}(t+1,t) = \frac{x_2(t+1)}{x_3(t)}\,[1.5 + x_2(t+1)\,\{1.5 + 0.015\,x_1(t)^{-3}\,x_2(t)^{-1.5}\}], \tag{14.6}$$

$$s_{31}(t+1,t) = \frac{x_3(t+1)}{x_1(t)}\,[-1.5 - x_3(t+1)\,\{150\,x_1(t)^3\,x_2(t)^{1.5} - 1.5\}], \tag{14.7}$$

$$s_{32}(t+1,t) = -\frac{x_3(t+1)}{x_2(t)}\,[150\,x_1(t)^3\,x_2(t)^{1.5}], \tag{14.8}$$

$$s_{33}(t+1,t) = \frac{x_3(t+1)}{x_3(t)}\,[1.5 + x_3(t+1)\,\{150\,x_1(t)^3\,x_2(t)^{1.5} - 1.5\}]. \tag{14.9}$$

And, at equilibrium, the diagonal elements of the Jacobian (response) matrix are:

$$s^*_{11} = x_1^{*2}[-1.5\,x_1^{*0.5}\,x_2^{*1.5}\,x_3^{*-1.5} - 0.015\,x_1^{*-2.5}\,x_3^{*-1.5}], \tag{15.1}$$

$$s^*_{22} = 1.5, \tag{15.2}$$

$$s^*_{33} = 1.5 + x_3^*\,[150\,x_1^{*3}\,x_2^{*1.5} - 1.5]. \tag{15.3}$$

At least one, in this case s^*_{22}, of these slopes is at equilibrium, always greater than one, no matter the eigenvector. Thus a required stability condition is met, which precludes point attractors or limit cycles. This leaves only the possibility for toroidal flow, or strange attractors (or various forms of chaos) to occur. The specific conditions discriminating between quasi-periodicity, strange attractors-containers, and other forms of chaotic motion are still to be derived. They must, among other things, involve the initial perturbation.

Not all initial states within the Möbius triangle, under the above parameter specifications, result in a ring-type quasi-periodicity. For example, along the line found at the intersection of the $x_1 = 0.2$ and $x_1 + x_2 + x_3 = 1$ planes, there is a well defined segment where the ring occurs. This segment commences at the neighborhood of the starting value point $[x_1^{(1)}(0) = 0.2,\ x_2^{(1)}(0) = 0.1956685\ldots,\ x_3^{(1)}(0) = 0.6043315\ldots]$, and ends at the vicinity of the point $[x_1^{(2)}(0) = 0.2,\ x_2^{(2)}(0) = 0.697\ldots,\ x_3^{(2)}(0) = 0.103\ldots]$. There are two basins of attraction in this case. At the transition points, a stable two-period cycle is transformed into the ring attractor. Thus, there seems to be a secondary locking phase involved in the phase portrait associated with starting values along a primary locking phase. The secondary locking phase is associated with parameter values. In this case the intermediate locking involves, at least, an attracting two-period cycle.

Clues as to the inner structure of this attractor are given by the four legs attached to the ring close to its four corners and created at the start up of its formation, when the initial point is either inside or outside the ring-attractor. The four legs reveal the starting phase of a rotating four-period cycle, the first time ever such event has been revealed in socio-spatial dynamics. A type of Cantor set is behind the process. These four legs, revealed in the motion shown in Figure 1, constitute the structure of the ring-attractor. Each leg contains a track moving toward the ring from some starting position $[y^{(1)}(0), y^{(2)}(0), y^{(3)}(0), y^{(4)}(0)]$. These initial points of the

four legs are the first four points of the map's rotating four-period cycle

$$y^{(1)}(0) = [x_1(0), x_2(0), x_3(0)],$$
$$y^{(2)}(0) = [x_1(1), x_2(1), x_3(1)],$$
$$y^{(3)}(0) = [x_1(2), x_2(2), x_3(2)],$$
$$y^{(4)}(0) = [x_1(3), x_2(3), x_3(3)],$$

in the Möbius triangle.

The ring is formed in phases. In a clockwise movement the rotating four-period cycle fills the space among the four legs of the ring-attractor with a smooth rotation, as shown in Figure 2. During the first phase the space among the jets is split into 26 (2×13) sub-spaces of approximately equal first phase bands. In total, there are $2^3 \times 13 = 104$ such bands on the ring. The process strongly resembles the formation of a Cantor type set, in an arithmetic sequence from a toroidal motion.

These bands having been marked, the second phase commences. Each first phase band is split into 14 (2×7) approximately equal second phase bands. A total of $2^4 \times 7 \times 13 = 1,456$ second phase bands now constitute the ring-attractor. After all 1,456 bands have been scanned by the rotating four-period cycle, the next phase commences.

During this phase, third phase bands are formed, by having the rotating four-period cycle split each second phase into three third phase bands for a total of $2^4 \times 3 \times 7 \times 13 = 4,368$ bands. Now the filling of each band occurs by having the four-period rotating cycle jumping every three third level bands. In other words, at this stage, the movement of the rotating four-period is no longer continuously spanning bands in each of the ring-attractor's four legs. Instead, it moves discontinuously.

Due to limitations in the software used, the fourth phase in successively banding the ring could not be observed, and the process of non linear arithmetic diffeomorphisms generating the Cantor-type sets could not be precisely established. Watching the formation of the ring, while lines are drawn, indicates that the rotation of the four-period cycle is counter-clockwise, while the lines of the cycle move clockwise.

Moving toward the ring from the inside, the rotating four-period cycle forms an envelope to an ellipsoid inside the ring, partly having formed in Figure 2. The ring acts as a "container" retaining the movement of the rotating four-period cycle when the initial values are inside the eventual ring. An ellipsoid is also formed when the initial values are outside the ring as well.

Periodic analysis of the ring structure and experiments with different time lags indicate that the periodicity in the rotation is robust, as expected. It is present in both, the time-one Poincaré sections and associated circle maps, no matter the lag involved or the period forced on its rotation. Poincaré sections always show the invariant circle. Thus, it seems that a strong conservation principle must apply and the presence of a, still to be derived, Hamiltonian must be sought. A similar finding is also detected in the second quasi-periodic case, as it will be seen later.

Figures 3–6 show the Poincaré section of a one-dimensional (variable) map and its corresponding circle map for putative forcing equal to one, and time lag equal to two, Figure 3 (Poincaré section) and Figure 4 (its circle map). For an identical putative forcing and a time lag equal to four time units, see Figure 5 (Poincaré section) and Figure 6 (its circle map).

5. BLACK HOLE: AN ASYMPTOTICALLY STABLE POINT

This case represents a hybrid between a nodal fixed point attractor and periodic toroidal flow. It contains fractal dimensions and resembles a "black hole." It can be transformed, through a bifurcation involving changes in parameter values, to a limit cycle type, quasi-periodic dynamic shown in the next section. The attractor contains an asymptotically and cyclically reached fixed point at the center of mass, which is very slowly approached through a complex spiraling motion.

For any initial value $[x_i(0);\ i = 1, 2, 3]$ within a sharply defined boundary in the phase portrait, the map converges toward the "hole" as shown in Figure 7, tracing different spirals with each initial value; see also Figure 8, where lines are drawn. Shade in Figure 7 indicates well defined areas of different speeds in motion. Regions with different speeds of movement are very sharply

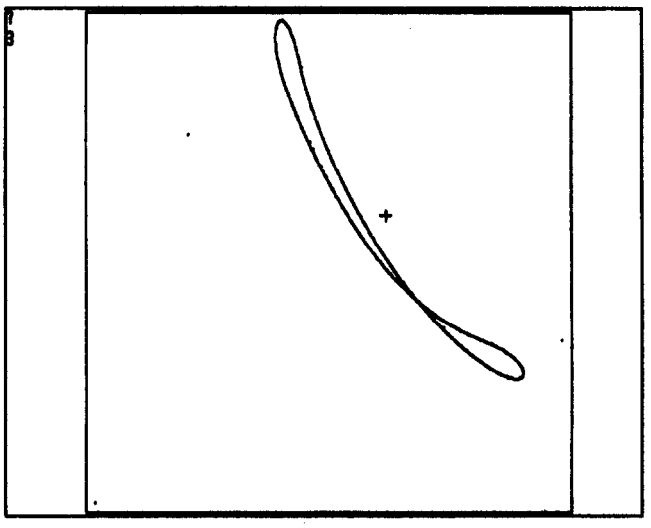

Figure 3. The Poincaré section of the rectangular ring attractor with a time lag equal to two iterates.

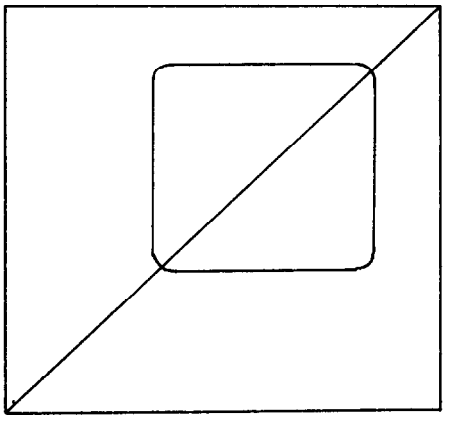

Figure 4. Circle map of the ring attractor under a time lag of two iterates.

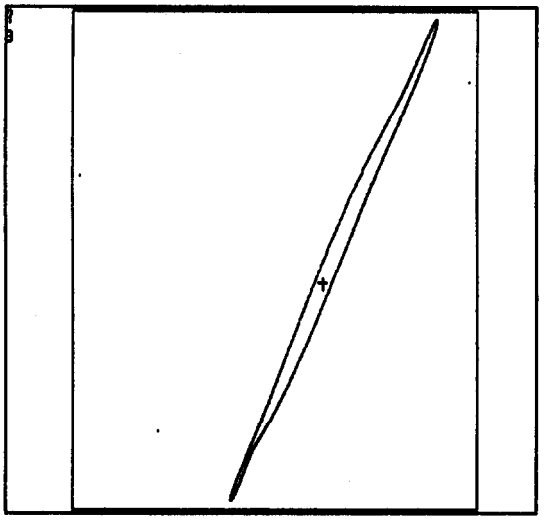

Figure 5. Poincaré section with a time lag equal to four iterates.

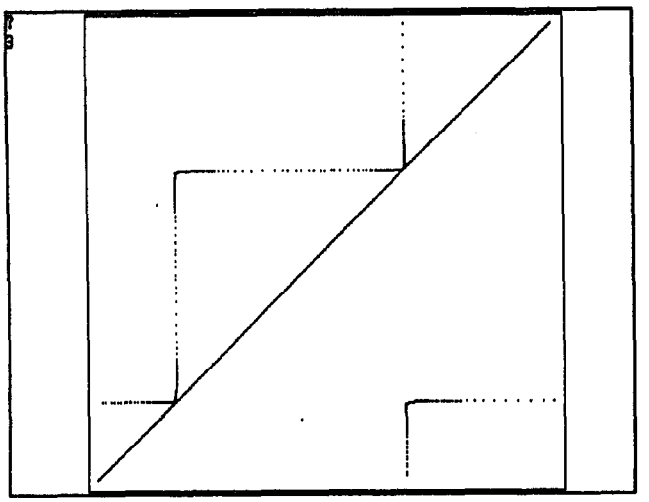

Figure 6. Circle map of the ring with time lag equal to four iterates.

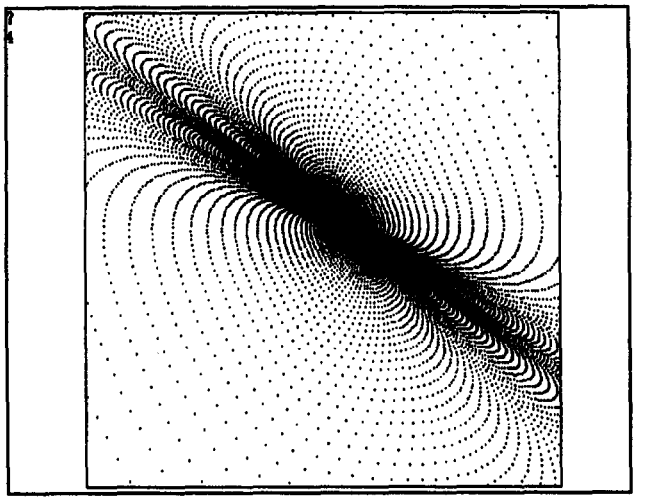

Figure 7. A black hole type point attractor, when points are drawn.

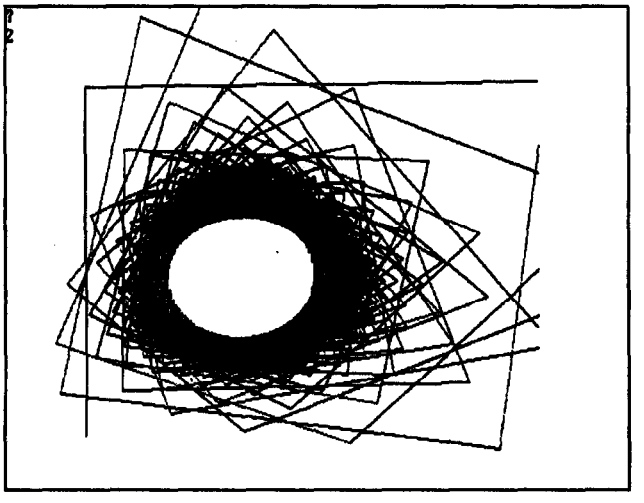

Figure 8. The black hole point attractor, when lines are shown.

delineated, with a rather low velocity along the core of a NW-SE axis in an ellipse shaped area with its center of gravity at the location of the hole.

Each point on this trajectory seems to belong to a very large number of distinct sink spirals pointing toward the hole. Moving closer toward the point attractor, the space is filled at a slowing pace. The example shown corresponds to starting values of $[x_1(0) = 0.2, x_2(0) = 0.5, x_3(0) = 0.3]$. The hole is located at the neighborhood of the point $(x_1^* = 0.126717, x_2^* = 0.546566, x_3^* = 0.326717)$.

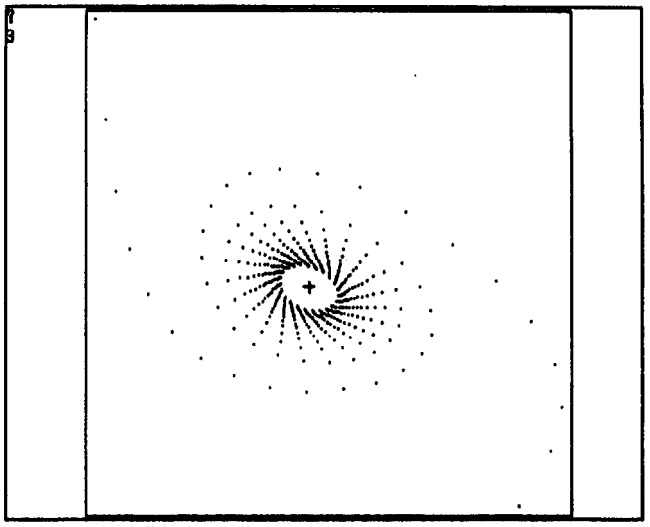

Figure 9. Poincaré section of the point attractor, under a 5-period putative forcing: a decrease in the number of spiral arms is shown.

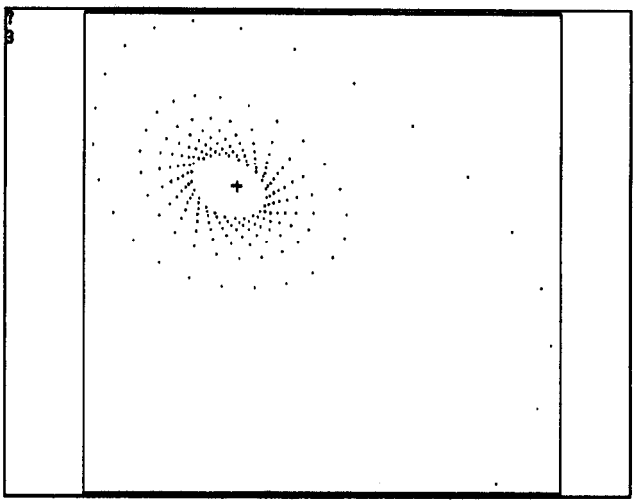

Figure 10. Poincaré section, under a 10-period putative forcing: one spiral arm with fractal dimensions.

A series of magnifications indicates clearly the presence of a fractal dimension; see Appendix for its definition. As the resolution of observing the black hole increases and by moving closer to the core, the overall pattern showing a series of folding sink spirals is maintained. The pattern indicates that each point on the surface belongs simultaneously to many spirals, all converging (at various angles) toward the hole.

Periodic analysis of this trajectory reveals the presence of two distinct spiral arms in the case of a five-period putative forcing and in the one-time-lag Poincaré section, Figure 9. It shows one spiral arm, within which many spiral motions can be traced, in a ten-period putative forcing

and under the same lag's Poincaré section, Figure 10. This analysis reveals that the black hole's dynamic path is traced by a single trajectory containing ten spiral arms, although the points' position seem to form a very large number of "illusionary" spiral arms. Only 2,000 points are shown in Figures 9 and 10.

Of particular interest is the phase portrait of this "black hole"-type fixed attractor. The dynamics associated with this particular parameter set (Appendix, case ii) contain only two types of motion: either a fixed attractor in all three locations, or a stable two-period cycle on two locations and a fixed attractor in the third location. A seemingly sharp border splits the two domains. Numerical simulation with a series of different starting values on a line found at the intersection of the $x_1 + x_2 + x_3 = 1$ plane with the $x_1 = 0.1$ plane, reveals the following: at approximately $\bar{x}_2(0) = 0.302695\ldots$ and at $\bar{x}_3(0) = 0.597305\ldots$, the regime which results in a black-hole type fixed attractor commences. A stable two-period cycle is recorded up to $x_2(0) \leq \bar{x}_2(0)$, and consequently, $x_3(0) \geq \bar{x}_3(0)$, given that $x_1(0) = 0.1$.

How the "black hole" is formed and captures all trajectories at $[x_1(0) = 0.1, \bar{x}_2(0), \bar{x}_3(0)]$ is shown in Figure 11, where the discrete dynamic path's lines are traced. Apparently, from a stable two-period cycle involving a motion among two initially attracting points, the trajectory slides gradually toward a third attractor. This attractor is found in the region where the black hole is located, in the triangular area of the two-dimensional space (the Möbius triangle). When the trajectory moves close enough to the hole's attracting field, the gravitational force grabs it.

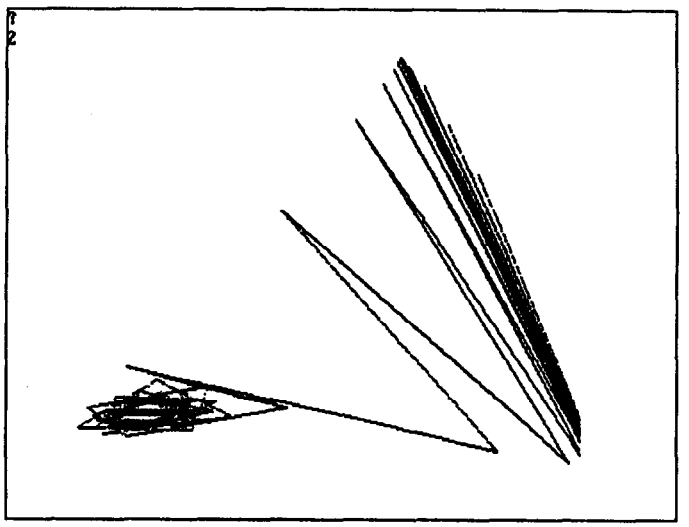

Figure 11. The capturing of the iterative process' trajectory by the strong attractor, given a starting value away from it.

This event reveals the presence of bifurcating behavior involved in starting states. Thus, chance through the initial perturbations (i.e., start up conditions) play a significant role in the dynamics involved and the types of evolutionary paths possible for the system to encounter. In this case the bifurcation is quite simple: a stable combination of a fixed point and a two-period cycle is transformed into an elaborate (asymptotically reached through a spiral motion) fixed point attractor.

Transition from a fixed point and a two-period cycle into a "black hole"-type attractor is only one of many kinds of evolutionary transitions possible in the universal map. This one is recorded in a phase portrait. Sequences of phase portraits conceal also evolutionary events. Attributed to changes in the environmental parameter set $[A]$, or in the elasticities of comparative advantages set of exponents $[a]$, many more types of evolutionary transitions may occur. Each of these bifurcations involves a distinct and different transition.

A ring to hole dynamic transition is a Neimark type bifurcation, see [12], in the three-dimensional version of the map at the "flutter" boundary where a cycle loses its stability. Qualitatively similar to that is the fixed point from a limit cycle transition involved in the Hopf bifurcation of continuous dynamics. This is the bifurcation where an equilibrium point loses its stability.

This transition is also equivalent to that found when a fixed point switches into a two-period cycle in the two-location one-stock specification of the discrete relative dynamics, i.e., the flip bifurcation. The next case, a spinning drop type quasi-periodicity, is also a generalized version of a point attractor to a limit cycle transition found in the Neimark, Hopf and flip bifurcation. A black hole is transformed into a spinning drop through a bifurcation involving only the exponents [a]. The precise intermediate steps between the two dynamics are still to be analytically specified.

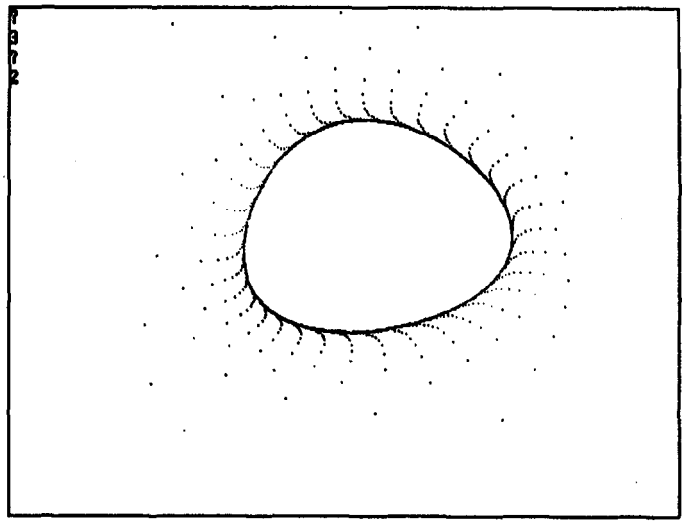

Figure 12. The spinning drop-type attractor, when points are shown.

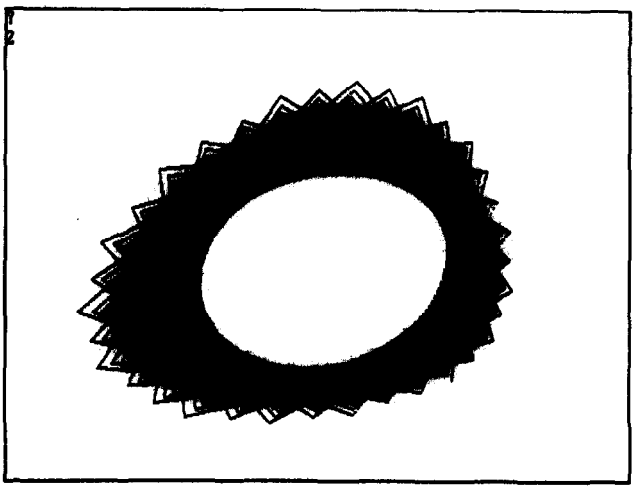

Figure 13. The drop-attractor, when lines are drawn. Starting values are outside the attractor.

6. SPINNING DROP

This case of quasi-periodicity is more complex than that of Section 4 identifying a "rectangular ring." In Figures 12 (points) and 13 (lines) the case of an attractor is shown, seemingly resembling a drop falling into a liquid while spinning, under the initial conditions [$x_1(0) = 0.2, x_2(0) = 0.5$, $x_3(0) = 0.3$] found outside the ring; 20,000 interations are shown. Specifications regarding the parameter values are given in the Appendix.

The inner structure of this attractor only slightly resembles that of the ring attractor. There are significant differeces on how the two are formed, i.e., in the instructions of deriving the two Cantor-type sets. Whereas the ring attractor of Section 4 contained four legs-tracks, the drop attractor has $2 \times 17 = 34$ jets.

During the first phase of the drop ring-attractor formation a rotating four-period cycle spans the initial 34 legs in jumps of nine. After a complete rotation, the cycle has span 36 legs, so that the begining of the next cycle commences at the third leg. In the first phase of the drop attractor formation, each of the 34 first phase bands split into either eight or seven sub-bands. Seventeen legs have eight, and seventeen have seven bands, so that an eight first level band jet is followed by a seven first level band jet. In total, there are 255 first level bands in all initial 34 jets of the drop attractor.

At the second phase, 128 first level bands are split into eight second level bands and the remaining 127 first level bands are split into seven second level bands for a total of 1913 second level bands. Eight bands at the second level first-level-band is followed by seven bands at the second level first-level-band. During the next phase, each of the second level band is split into four third level bands for a total of 7,652 bands. Software limitations do not allow for further observing the formation of the set on the drop attractor. A peculiarity of this attractor is that, as the second level banding process takes place, spikes are observed: i.e., points slightly off the attractor appear. Their purpose and cause are still unknown, possible related to the resolution of the computer screen, or the machine's approximations.

Periodic and lagged analysis of this attractor seem to demonstrate the presence of a conservation principle. The rotation of the four-period cycle is robust with reference to both lags and forced periodic movement. While in the case of the ring attractor of Section 4 periodic putative forcing or lagged iterates do not reveal a period greater than a four-period cycle, in the case of the spinning drop attractor a number of periods are detected. They range from a three-period up to a 17-period cycle, including both odd and even periods.

Limited analysis with respect to the initial conditions in the phase portrait of the Möbius triangle seems to indicate that the spinning drop atttractor is the only event occurring in the triangle. There seems to be no other basin of attraction in this case.

7. DISCUSSION

By looking at these three cases one thing becomes immediately apparent. Their intrinsic value, if any, lies not so much on the detail that they provide, regarding the possible dynamic paths of the populations, but on their inner form. Details about the dynamics of interacting populations, in accordance with the map's specifications and subject to the specific environmental and initial comparative advantages, are too specific to be of any real significance. Instead, the worth of these iterations possibly lies in the processes giving rise to these dynamics and in their variety. Thus, the bulk of the discussion which follows is on the broader aspects of these three cases, having to do with the imprinted mechanisms of evolution found to govern these three cases at hand.

In all three cases presented, it is clear that the end-state by itself does not convey the total picture of their inner structure and formation. By looking at the choreography of these spatio-temporal patterns from start to finish, one obtains, not only hints about their dynamics but, more importantly, one can identify the mechanism of order present in shaping their final stage.

The scenario unraveled provides tell-tale signs of the evolution of these forms when traveling through the parameter or starting value space and by following the attractors. Even in absence of exact knowledge regarding the specific kinetic conditions, one could tell something about the future states of the iterative process, given some knowledge of certain initial iterates and temporal proximity to the future state. Of course, all critically depends on how close the path of the travel is to thresholds of transition in both the parameter and starting values space. And it also depends on the confidence one has, regarding the instructions in forming Cantor type sets in quasi-periodicity, or asymptotic fixed-point behavior, imprinted in the specific kinetic conditions of the map.

Evolution, in form of the three cases discussed here, occurs by having the iterative process undergo transitions by either moving through the parameter space, or by changing starting values. As a result, certain fundamental bifurcations in elementary forms occur. The elementary geometry of these three-location specifications of the relative geography map are: the stable or unstable fixed point; all stable or unstable, even or odd, period cycles; and a combination of the two.

A higher order asymptotically stable fixed point attractor in the Möbius triangle of the universal map of relative dynamics is the black hole with fractal dimensions. A higher order limit cycle is any attracting-ring type of quasi-periodicity, a Cantor set formed by a rotating periodicity. One may consider this rotation to be a morphogenetic principle in developmental dynamics of form.

Thus, by changing (decreasing) parameter values for a_{31}, to $a_{31} = -1.5$ (rectangular ring) from $a_{31} = -0.5$ (black hole), and by keeping the starting values unchanged, one switches from a point attractor- to a ring attractor-type quasi-periodicity. By further changing (decreasing) parameter values for a_{21}, to $a_{21} = 0.5$ (spinning drop), from $a_{21} = 1.5$ (black hole), one switches a point attractor into another type of ring attractor of quasi-periodicity. Switching a (fixed) point attractor with fractal properties into quasi-periodicity is one of the fundamental bifurcations found in the universal map. This bifurcation is another morphogenetic principle of evolution in form.

Changes in the model's elasticities have concrete meaning: for each location i, the sum of its corresponding row entries in the elasticities matrix $[a_{ij}]$ identifies the total effect that location i has on all three locations. The column total, on the other hand, identifies the effect that all other locations have upon j. By changing the elasticity a_{31} a shift from the rectangular ring to the black hole results. One may attribute this shift to the effect location "3" now has on all locations as its total impact increased from -3 to -2, while the effect of all locations on "1" increased from 0 to 1. Equivalently, changing the elasticity a_{21}, and shifting from a black hole to the spinning drop, one may attribute the switch to the decreased effect from 1.5 to 0.5, location "2" now has on all locations, and the decreased effect, from 1 to 0, all locations have upon location "2."

Phase switching follows, with changes in the very slow moving elasticities (i.e., the exponents) of the discrete map, while keeping constant the values of the parameters depicting the environment (the relatively slow moving scale parameters of the map which are assumed to change faster than the exponents). It also occurs with changes in the fixed values or initial perturbations in the state variables. Qualitatively, this fundamental bifurcation is equivalent to: (a) the Hopf bifurcation of continuous two-dimensional dynamics, switching a fixed point through a center to a stable limit cycle; and (b) to the Dendrinos-Sonis discrete two-dimensional relative dynamics (flip type) bifurcation, switching a fixed point through a center, to a stable two-period cycle.

One of these geometries-geographies is the black hole-type point attractor, revealing a specific type of fractal dimension: no matter how close one moves towards the center (the point attractor), and, consequently, no matter the increase in the resolution used to observe it, as long as the point remains at the center of the pattern chosen to observe it, the picture remains qualitatively unaltered. A large number of spiralling arms are always shown swirling toward the focal point. They are recorded by a single trajectory in the Möbius triangle. In this case, the informational dimension d_I (see Appendix) is unaltered. A continous folding of spirals is observed. Fractal dimension is an elasticity measure: it identifies the constant rate of change in any measure of the pattern under analysis, given a unit change in the magnification of resolution. In socio-spatial geometries this must be rather rare.

In two of the cases presented, specifically the two-ring attractor quasi-periodicity, and for appropriate initial conditions, relatively large hollows of space in the Möbius triangle are observed. These ellipsoids represent inaccessible regions of relative population allocations impossible to attain, under these model specifications and values for $[a]$ and $[A]$. On the other hand, there are certain very narrow bands of space, associated with rather strong and robust attractors, toward which relative population distributions gravitate. If it is not possible to identify them in real socio-spatial dynamics, then their inner mechanism (quasi-periodicity) may give reasons why. Simply put, quasi-periodicity may not be observable in real socio-spatial systems, partly because it may be a rare event.

By exploring the general and abstract universal map of model socio-spatial dynamic behavior, one comes across forms of order in a seemingly chaotic but deterministic motion. Often these forms have recognizable patterns, like the "black hole" of Section 5 and the "spinning drop" of Section 6. Most frequently, however, new patterns of order and, thus, spatio-temporal novel forms are revealed, like the "rectangular ring" case of Section 4, a widespread occurrence in the three (and four) dimensional version of the one-stock three-location map.

These patterns exhibit an intrinsic aesthetic quality, both in their end-state and their developmental paths toward the end-state. Of interest from an epistemological stand point, could be the fact that an astonishingly simple set of instructions imprinted in the universal map can fill the regions of its parameter and initial states space with a wide range of performance. In the theatre of this state variable space and associated Poincaré sections and circle maps, the menu of performance is unparalleled by any known discrete or continuous map. Use of this map is not confined to aesthetic or mathematical interest, however. The new concept of a "roatating four-period cycle" emerging from the inner structure in two of the cases presented will be addressed, next as to interpretations and implications it may hold for socio-spatial dynamics. Movement of the smoothly or jumpingly rotating four-period cycle may point to an inherent developmental inertia in population changes. It hints that, while under a particular band of a phase on the attractor, the population dynamics may entail very small changes in their relative spatial sizes. During these phases, the various transaction spatio-temporal costs may keep the relative size of these locations rather stable, the more so, the lower the phase of banding in the attractor-ring.

But in these phases always lurk even lower level phases of banding, as a result of the rotating motion of the four-period cycle. These could entail drastic developmental changes in relative population shares. During these transitions, transaction costs may not matter that much. It is underlined that these transitions do not involve any changes in any parameter or starting conditions. Thus, they are not evolutionary but simply developmental. Another set of complications emerges, thus, in the bifurcation menu of socio-spatial dynamics, where development as well as evolution may be affected by discontinuities, although no phase transitions are involved. Certainly, this unexpected realization must not be the last. Further exploration into the map's behavior is likely to unravel many more suprises.

8. CONCLUSIONS

Evolution of form obeys transformations following three elementary types of change: first, a change in the initial perturbation (starting state); second, a change in the slowly moving environmental parameters [A]; and third, a change in the very slowly altered elasticities in comparative advantages exponents [a].

Some of the evolutionary changes are smooth and progressive; others are abrupt, discontinuous and sharply different in form. A three part story of evolution is thus told by this universal map, depending on what change (or combination thereof) may be fueling it!

Attention was drawn to a generalized bifurcation in this three-dimensional case: it involved three specific points in the [a]-space, under fixed A's and starting values. A black hole type singularity was found to depict an elaborately formed point attractor; a "spinning drop"- and a "rectangular ring"-type attractor with quasi-periodicity were found to depict a form of limit cycle. A bifurcation was thus identified, which converts a black hole into either a spinning drop or a rectangular ring attractor, through a set of undetermined yet intermediate phases.

Both rings were found to be quasi-periodic, formed differently by a rotating cycle. Elementary forms and fundamental bifurcations were detected in this model geography-geometry. They provided clues as to the inner-structure of quasi-periodicity. It was alluded that the presence of quasi-periodicity and its underlying order may be necessary components for form to exist and for evolution in form to occur.

REFERENCES

1. D.S. Dendrinos, Theoretical developments in discrete maps of relative spatial dynamics, Presented in the *1987 Meeting of the European Regional Science Association,* Athens, August; appeared in *Systemi Urbani* **2/3** (1988).
2. D.S. Dendrinos, Volterra-Lotka ecological dynamics, gravitational interaction and turbulent transportation: An integration, Presented at the *1988 Meeting of the North American Regional Science Association,* Toronto; *Sistemi Urbani* (1991).
3. D.S. Dendrinos, Turbulence in congested spatial interaction dynamics, Presented at the *1989 Meeting of the European Regional Science Association,* Cambridge. UK; *Sistemi Urbani* (1991).
4. D.S. Dendrinos, Turbulence and fundamental urban/regional dynamics, Report No. SES-8216620, National Science Foundation, Washington D.C. (1984).

5. M. Sonis and D.S. Dendrinos, A discrete relative growth model: switching, role reversal and turbulence, Presented at the *Sixth Advanced Studies Summer Institute of the Regional Science Association*, Bamberg FRG; in P. Friedrich and I. Masser (eds.), *International Perspectives of Regional Decentralization*, Nomos, Baden-Baden (1987).
6. R. Reiner, M. Munz, G. Haag and W. Weidlich, Chaotic evolution of migratory systems, *Sistemi Urbani* **2/3**, 285–308 (1986).
7. D.S. Dendrinos, On the incongruous spatial employment dynamics, In *Technological Change, Employment and Spatial Dynamics*, P. Nijkamp (ed.), Springer Verlag, Berlin, pp. 321–339, (1986).
8. P. Nijkamp and A. Reggiani, Theory of chaos in a space-time perspective, *Mimeo, Department of Economics*, Free University of Amsterdam (1988).
9. R. Day, The emergence of chaos from classical economic growth, *Quarterly Journal of Economics* **98**, 210–213 (1982).
10. W. Barnett, J. Geweke and K. Shell (eds.), *Economic Complexity Chaos, Sunspots, Bubbles and Nonlinearity*, Cambridge University Press, (1989).
11. D.S. Dendrinos and M. Sonis, *Chaos and Socio-Spatial Dynamics*, Springer Verlag, New York, (1990).
12. J.M.T. Thompson and H.B. Stewart, *Non Linear Dynamics and Chaos*, John Wiley, New York, (1986).
13. W.M. Schaffer, G.L. Truty and S.L. Fulmer, *Dynamical Software: User's Manual and Introduction to Chaotic Systems*, Dynamical Systems, Inc., Tucson, (1988).

APPENDIX

Three Cases in Socio-Spatial Dynamics

The three particular points in the parameter space, which generate for particular initial conditions the following three forms correspondingly, are:

Rectangular ring:

$$A_1 = A_2 = 1, \qquad A_3 = 0.01,$$
$$[a_{ik}] = \begin{bmatrix} 0 & 0 & 0 \\ 1.5 & 1.5 & -1.5 \\ -1.5 & 0 & -1.5 \end{bmatrix}.$$

Black hole:

$$A_1 = A_2 = 1, \qquad A_3 = 0.01,$$
$$[a_{ik}] = \begin{bmatrix} 0 & 0 & 0 \\ 1.5 & 1.5 & -1.5 \\ -0.5 & 0 & -1.5 \end{bmatrix}.$$

Spinning drop:

$$A_1 = A_2 = 1, \qquad A_3 = 0.01,$$
$$[a_{ik}] = \begin{bmatrix} 0 & 0 & 0 \\ 0.5 & 1.5 & -1.5 \\ -0.5 & 0 & -1.5 \end{bmatrix}.$$

It is noted that in all three cases the environmental (scale) parameters A, as well as initial conditions, remain the same. The case of Section 5 is derived from the case of Section 4, by only changing the exponent a_{31} from -1.5 to -0.5; the case of Section 6 is derived from the case of Section 5, by only changing exponent a_{21} from 1.5 to 0.5.

All simulations shown in this paper used the Dynamical Software I.4 of W.M. Schaffer et al., [13]. They were carried out on an IBM PS/2, model 60, type 8560.

Analytically, the slopes-entries of the Jacobian matrix are given, see [11, Part III], by:

$$J = \|s_{ij}(t+1,t)\| = \left\| \frac{\partial x_i(t+1)}{\partial x_j(t)} \right\| = \left\| \frac{x_i(t+1)}{x_j(t)} \left[a_{hj} - \sum_{h=1}^{3} a_{hj}\, x_h(t+1) \right] \right\|,$$

which, at the (unstable) equilibrium, produce:

$$J^* = \left\| s^*_{ij} \right\| = \left\| a_{ij} - \sum_{h=1}^{3} a_{hi}\, x^*_h \right\|; \qquad i,j = 1,2,3.$$

These entries result in a set of eigenvalues for the various eigenvectors at the (multiple) equilibria the time-one map may have. Which one of these eigenvalues at each eigenvector is operative depends on the initial conditions,

among other factors. The above system's characteristic polynomial and eigenvalues, λ, are the result of the Jacobian condition:

$$\det \begin{vmatrix} s_{11}^* - \lambda & s_{12}^* & s_{13}^* \\ s_{21}^* & s_{22}^* - \lambda & s_{23}^* \\ s_{31}^* & s_{32}^* & s_{33}^* - \lambda \end{vmatrix} = 0,$$

which supplies, in turn:

$$(s_{11}^* - \lambda)(s_{22}^* - \lambda)(s_{33}^* - \lambda) + s_{12}^* s_{23}^* s_{31}^* + s_{13}^* s_{21}^* s_{32}^* - s_{13}^* s_{31}^* (s_{22}^* - \lambda) - s_{23}^* s_{32}^* (s_{11}^* - \lambda) - s_{12}^* s_{21}^* (s_{33}^* - \lambda) = 0.$$

The three roots of the characteristic polynomial define the values of the three eigenvalues associated with each equilibrium point. In this case of relative dynamics, always one of the eigenvalues is zero.

Rotation Number

The rotation number ρ is given by the expression, see [13]:

$$\rho = \lim_{T \to \infty} \frac{1}{T} \sum_{t=1}^{T} \frac{\rho(t)}{2\pi},$$

where T is the number of iterations and $\rho(t)$ is the number of revolutions needed to cover each period. If the movement is quasi-periodic the sequence never repeats exactly, thus, the number is irrational. On the other hand, if there is a periodic movement, then ρ is equal to the stable period cycle found in the dynamics.

Fractal dimension

Among the many definitions of fractal dimension, the informational dimension seems to be very appropriate for the black hole-type attractor. This dimension is given by:

$$I(e) = -\sum_i \rho_i \ln \rho_i,$$

where e is the dimension of a square on the Möbius triangle and i is an index of square on the phase portrait. Then:

$$d_I = \lim_{e \to 0} \left[\frac{I(e)}{\ln(1/e)} \right].$$